PERGAMON

Chemical Engineering Science 56 (2001) 3549–3561

Chemical Engineering Science

www.elsevier.nl/locate/ces

Clogging of fibrous filters by solid aerosol particles Experimental and modelling study

D. Thomas[a,*], P. Penicot[a], P. Contal[a], D. Leclerc[a], J. Vendel[b]

[a]LSGC-CNRS, Université Henri Poincaré, 1 rue Grandville – BP 451, 54 001 Nancy Cedex, France
[b]CE Saclay, DPEI/SERAC/LECEV, Bâtiment 393, 91 191 Gif-sur-Yvette, France

Received 1 April 1998; received in revised form 24 January 2000; accepted 20 August 2000

Abstract

A fibrous filter is a common cleaning device often used to remove particles from industrial gas streams. The main question which often arises concerns the evolution of the pressure drop and the filtration efficiency during the filter clogging. In the present study, the loading characteristics of HEPA filters have been studied experimentally. The increase of pressure drop and filter efficiency was measured and was linked to both the penetration profile inside the filter bed and the deposit structure observed thanks to scanning electron micrograph. We have also studied the influence of various parameters such as air velocity, particle size, aerosol concentration and filter main characteristics. A depth and surface filtration model has been developed based on the distinction between the fibres of the filter and deposited particles resulting in additional fibres inside the filter or on the filter surface. We can notice a good agreement between model and experiment. Moreover, model very well describes the transition area between depth filtration and cake filtration. This transition from one type of filtration to another is a continuous process. Model describes also the exponential decrease of penetration profile. © 2001 Elsevier Science Ltd. All rights reserved.

Keywords: Pressure drop; HEPA filter; Aerosol; Filtration; Clogging; Solid particles; Efficiency

1. Introduction

Fibrous filters (high efficiency particulate air filters (HEPA)) are widely used in many applications such as nuclear, pharmaceutical, food and semi-conductor industries. Typically constructed of matted glass or quartz fibres, HEPA filters are designed to remove particles from the gas stream with efficiencies of at least 99.97%. They are used either to treat polluted air before it is released into the environment or to admit air with very low dust concentration into a process.

The two main characteristics of these filters are pressure drop and particle collection efficiency. These parameters depend on the structure of filters (packing density, fibre diameter, and thickness), on the operating conditions (filtration velocity, temperature) and on the characteristics of the filtered aerosols (density, particle size and distribution). In addition, pressure drop and efficiency are functions of filter loading.

Most of the published works mainly are concerned with clean filters but only few studies have been devoted to the evolution of the filter performance while clogging. To shed light on this aspect, we decided to carry out several series of filtration experiments according to different operating conditions. This paper aims at giving a better understanding of the loading process, and of the evolution of both pressure drop and efficiency. The influence of the operating conditions are well studied and models are compared with our experimental results.

2. Previous studies

2.1. Filter efficiency

Considering that the first stage for solving all problems entailed by aerosol particles filtration consists of

* Corresponding author. Fax: 33-383-32-29-75.
E-mail address: dthomas@ensic.inpl-nancy.fr (D. Thomas).

0009-2509/01/$ - see front matter © 2001 Elsevier Science Ltd. All rights reserved.
PII: S0009-2509(01)00041-0

a good description of the flow fields around fibres inside the filter, many investigators have focused on their modelling. Generally, filters are schematically depicted as a structure of "cells", each cell corresponding to a fibre roughly described by a cylinder surrounded by the fluid (Kuwabara, 1959; Happel, 1959). Other studies have been carried out (Spielman & Goren, 1968; Kirsch & Stechkina, 1977) using a fan model, (Lajos 1985; Nagel & Buggish, 1996; Brown, 1993) but subsequent aerosol filtration models are generally based on the "cells" model description.

Several investigators have developed their contribution to the study of clogging of fibrous filters thanks to an analysis of particles deposit structure. Billings (1966), Kanaoka and Hiragi (1990), Witten and Sander (1983) and Payatakes and Gradon (1980) have scrutinised the growth of particle dendrites on fibres. Those studies only enable a better understanding of the deposit process.

The clean filters removal efficiency E is closely linked to the single fibre collection efficiency η according to an expression obtained thanks to a mass balance on a filter element of thickness dz and integrated on the total filter thickness Z.

$$E = 1 - \exp\left[-\frac{4\alpha\eta Z}{(1-\alpha)d_f\pi}\right], \tag{1}$$

where α is the packing density defined as the ratio of the volume of fibres and the total filter volume.

A lot of authors have focused their efforts to estimate η, which depends on the collection mechanism involved in the filtration process: Brownian diffusion (especially concerning very small particles), interception and inertial deposition (concerning large particles). To each mechanism corresponds an expression η_y (for the mechanism y) generally a function of a dimensionless number characterising the mechanism. Let us quote the studies of Stechkina, Kirsch, and Fuchs (1969), Natanson (1987), Liu and Rubow (1990), Payet, Boulaud, Madelaine, and Renoux (1992) for Brownian diffusion, Kuwabara (1959), Lee and Liu (1982), Liu and Rubow (1990) for interception and Suneja and Lee (1974), Ilias and Douglas (1989), Gougeon (1993) for inertial deposition. As pointed out by Ramarao, Tien, and Mohan (1994) the fibre collection efficiency is the sum $\eta = \eta_D + \eta_R + \eta_I$, which therefore implies a large number of possible combinations. An alternative approach is to assume that the aerosol penetration defined by the quantity $(1-\eta)$ may be approximated by the product of penetration due to individual mechanisms: $(1-\eta) = (1-\eta_D)\cdot(1-\eta_R)\cdot(1-\eta_I)$. In gas filtration, the first approach is commonly used by assuming that each mechanism acts independently from one another.

2.2. Filter pressure drop

2.2.1. Pressure drop of clean filter

Davies' law describes the pressure drop evolution (ΔP) of a clean fibrous filter with filtration velocity (U_0).

$$\frac{\Delta P}{Z} = 64\mu U_0 \frac{\alpha^{3/2}(1+56\alpha^3)}{d_f^2}. \tag{2}$$

2.2.2. Pressure drop of clogged filter

A few attempts were made to give a mathematical prediction of pressure drop evolution during clogging: Davies (1973), Bergman, Taylor, and Miller (1978), Juda and Chrosciel (1970), Kanaoka and Hiragi (1980), Payatakes and Okuyama (1982), who all developed a theoretical model describing the pressure drop due to particles collected inside the filter and Novick et al. (1990) whose approach is quite different since he is the only one who takes into account the presence of a cake.

Davies' (1973) model is based on the expression he had developed for a clean filter. Therefore, he takes into account the collected mass supposing that particles uniformly settle on each fibre entailing an increase of the fibre diameter and filter packing density. The main advantage of this model is that all parameters may be easily calculated. Nevertheless, the particle size is not taken into account.

In Bergman's approach, two kinds of fibres contribute to particles collection inside the filter and to pressure drop: the initial clean fibres of the filter on one hand and the deposited particles forming dendrites which could be considered as new collecting fibres on the other hand. Then he modifies Davies' (1973) model including the particle size according to the following expression:

$$\Delta P = 64\mu U_0 Z\left(\frac{\alpha}{d_f^2} + \frac{\alpha_p}{d_p^2}\right)^{1/2}\left(\frac{\alpha}{d_f} + \frac{\alpha_p}{d_p}\right). \tag{3}$$

This model which is easy to use supposes a homogeneous deposition of aerosol particles inside the filter. Bergman et al. (1978) consider that particle deposit and particle diameter are uniform over the whole filter thickness. Nevertheless, Letourneau, Mulcey, and Vendel (1990) showed, by a peeling method, that collected particles are not uniformly distributed over the whole thickness of a filter. Surface layers are more loaded than depth layers. Later, Vendel, Letourneau, and Renaudin (1992) compared experimental results with the relation of Bergman et al. (1978) for the most penetrating aerosol (0.15 and 0.25 μm). They noted that this relation underestimates the pressure drop. Therefore, they suggested that filter pressure drop model as a function of the deposited aerosol mass requires the knowledge of the penetration profile of particles inside the filter medium. All the other models are not very easy to use, particularly to compare with the experimental data, since parameters they require are difficult to estimate. Kanaoka and Hiragi (1990), Payatakes and Gradon (1980) and Payatakes and Okuyama (1982) have established models based on the determination of the drag force acting on the fibres which is full of complexities. Juda and Chrosciel's (1970) model also raises problems of comparison with our experiments since several unknown constants are needed.

Novick et al. (1990) approach of the filter cake formation requires the knowledge of a parameter which is experimentally difficult to obtain: α_{pc}, cake packing density. He considers the pressure drop entailed by the clogged filter as the additional pressure drop of the clean filter (ΔP_0) and the one of the cake according to the following expression:

$$\Delta P = \Delta P_0 + k_2 U_0 m. \tag{4}$$

The expression for k_2 is: $k_2 = h_k a_g^2 \alpha_{pc} \mu / [C_c (1 - \alpha_{pc})^3 \rho_p]$ with h_k the Kozeny constant = 5 for spherical particles.

According to experiments several investigators have given a range for α_{pc} values. Kirsch and Lahtin (1975) found for a cake made of particles smaller than 1 μm, α_{pc} values in the range of 0.08–0.15. The same kind of study carried out by Schmidt and Löffler (1990) with 3.8 μm particles gave α_{pc} values between 0.11 and 0.21.

Thus, the purpose of this paper is to illuminate some of the issues involved in the field of the effect of particle loading on fibrous filters performance, to compare and to complete the conclusions of previous works with our results and finally to develop a new theoretical model in agreement with all our experimental data (pressure drop, penetration profile and filter efficiency).

3. Experimental set-up

Fig. 1 shows a schematic diagram of the experimental set-up. It consists of an aerosol generator, a filter holder containing the test filter, a dryer, a mass flowmeter and two aerosol sampling systems upstream and downstream the filter. The compressed air to the aerosol generator is dried through a refrigeration system. Aerosol particles penetrating the test filter are perfectly captured by a back-up absolute filter. Temperature and pressure are controlled at different points in the system. Air velocity inside the filter is kept constant using a flow control system and pressure drop across the filter is measured with a high accuracy differential pressure transducer. A computer enables data acquisition.

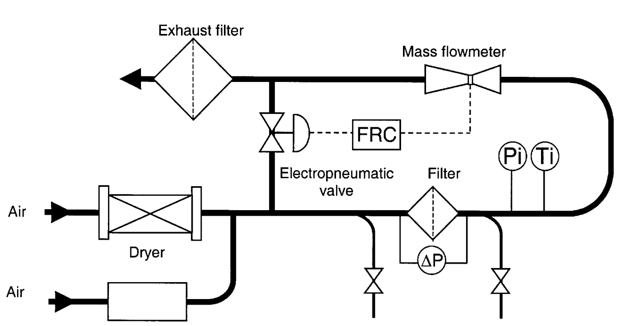

Fig. 1. Experimental set-up.

Table 1
Filters characteristics

Filter	Z (μm)	α	d_f (μm)
D 306	370	9.4×10^{-2}	1.3
D 309	575	5.6×10^{-2}	1.1

Generated solid particles came from a soda fluorescein aerosol. It is obtained by atomising a soda fluorescein solution whose concentration (10 or 100 g/l) entails modification of both particle size distribution and generated aerosol concentration. A standardised NFX 44-011 generator was used according to the following process. The aerosol is generated with a nebuliser operating at 1.8 bar. The aerosol stream from the nebuliser passes through two impactors in order to eliminate too large particles and becomes solid by introducing dry compressed air. Removing the second impactor from the generator enables another modification of both particle size and aerosol concentration. Particle size distributions were measured using a Differential Mobility Particle Sizer (DMPS TSI 3071) in line with a Condensation Nucleus Counter (CNC TSI 3020) and was found to be log-normal with the following mean diameters: 0.18, 0.31 and 0.40 μm (geometric standard deviation of 1.8 in each case) for D309 filter and 0.15 and 0.26 μm for D306 filter (geometric standard deviation of 1.6 in each case).

3.1. Filter characteristics

A HEPA glass fibre filter (reference D309) was used for all experiments. We have compared our model with our experiments and with Vendel experiments (on filter reference D 306). Its main features (thickness, packing density, fibre mean diameter) are detailed in Table 1. The thickness was measured observing the filter section thanks to scanning electron micrograph. Packing density was calculated from grammage and thickness. The fibre mean diameter was estimated using Davies' (1973) law. Thus, plotting the pressure drop entailed by an air flow passing through the filter against the air velocity, we obtain a straight line whose slope gives the product: $64\,\mu Z \alpha^{3/2}(1 + 56\alpha^3)\, d_f^{-2}$. All parameters are known in this expression except d_f.

3.2. Description of the experiments

The experiment consists in filtering generated aerosol while air velocity inside the filter is kept constant. The upstream and downstream aerosol concentrations are measured thanks to iso-kinetic samples on absolute fibrous filters. The deposited particles are quantified by fluorescence measurement after the sampling filters are washed with a pH 9 solution during 24 h. We have made sure that this period of time was sufficient for all soda fluorescein particles to be in solution. This method enables the aerosol concentration determination on a wide range from 10^{-11} to 10^{-6} g/cm^3. That way, we can calculate the filter efficiency varying with time.

Pressure drop is continuously measured along clogging. At the end of the experiment, the filter is weighed for the determination of the mass collected per unit of area. For a given set of filtration conditions, experiments are carried out repeatedly but with different time of exposure in order to obtain filters at various states of clogging. We can then plot the collected mass against filtration time and obtain a linear equation linking both parameters. Thus, the deposit and its evolution can be observed with help of scanning electron micrograph. Moreover, in this way, validation of the results is then ensured by the reproductibility of the experiments.

The last part of the experimental process consists in the determination of penetration profile inside the filter. Our simple approach is based on the use of adhesive tape pieces which enable to cut out an area of the filter into several slices. We make sure that the same strength is applied on each adhesive tape piece so that all slices are as uniform in thickness as possible. The fluorescence of particles deposited on each slice as well as the area of the piece of filter are precisely measured. The mass collected in the whole depth of the filter is in that way determined allowing the penetration profile description by plotting the ratio $R = m_{\text{slice } J}/\sum m_{\text{slice } J}$ against the depth inside the filter. Let us emphasise that the reproductibility of this approach was tested and found to be rather good. The accuracy of R was found to be around 8%.

4. Results

4.1. Evolution of the pressure drop during clogging in relation with the deposit aspect

Fig. 2 shows the evolution of pressure drop during clogging by soda fluorescein particles. It must be emphasised that the repeated experiments with different times of exposure give perfectly identical results testifying to their excellent reproducibility.

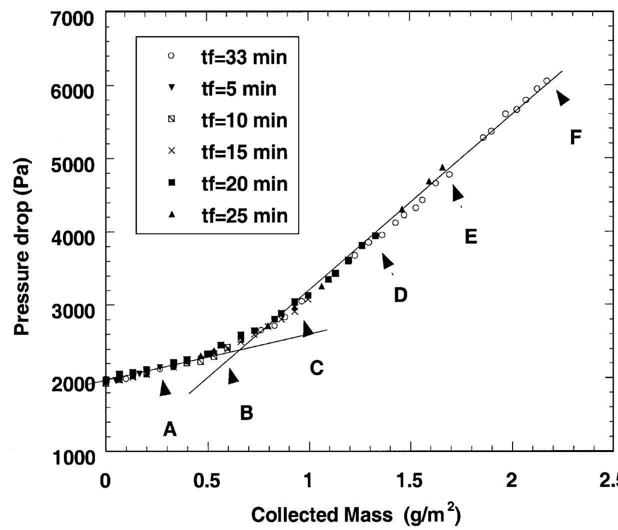

Fig. 2. An example of the evolution of pressure drop during clogging by soda fluorescein particles ($d_p = 0.18$ µm, $C = 3.5$ mg/m^3, $U_0 = 30$ cm/s).

Two steps may be distinguished in evolution of pressure drop as a function of collected mass. During the first step, the evolution is slow, whereas, in the second, the increase becomes markedly linear. These observations are in good agreement with the experimental results of solid monodisperse particle clogging of fibrous filters (Japuntich, Stenhouse, & Liu, 1994).

Scanning electron micrograph photographs (Figs. 3 and 4) of the loaded filter surface show the evolution of particles deposit during clogging. Photographs clearly suggest that at the beginning of filtration, particles are deposited in the depth of the filter (Fig. 3A and B) and form dendrites (Fig. 4A). Nevertheless, we can notice in the following photographs (Fig. 3C–E) that as loading increases fibres are less and less apparent. It corresponds to the formation of cake on the surface of the filter. More precise observations greatly show that for a heavy loading filter cake is formed on the front edge of the filter (Fig. 4B).

4.2. Penetration profile

Fig. 5 shows the penetration profile of soda fluorescein particles inside the filter. On this diagram, the ratio R(%) is plotted against the depth inside the filter for two values of the exposure time. Let us first notice the exponential decrease of the penetration profile from 0 µm corresponding to the loaded filter surface to 600 µm corresponding to the opposite side. Now comparing the two penetration profiles, we become aware that the first slice corresponds to 40% of collected particles for a weak loading, whereas it corresponds to 70% for a heavy loading. Moreover, the proportion of particles present in the depth of the filter

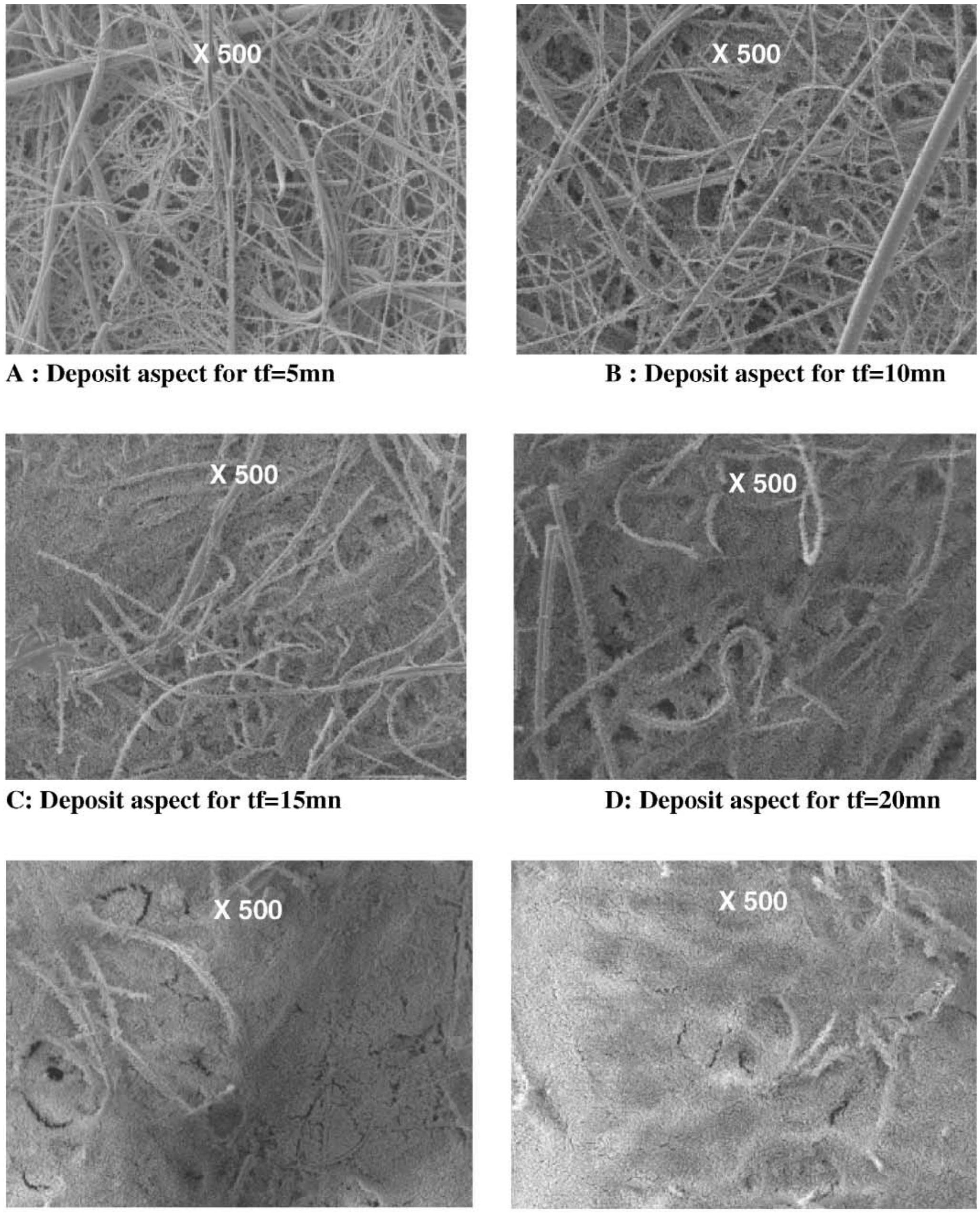

A : Deposit aspect for tf=5mn

B : Deposit aspect for tf=10mn

C: Deposit aspect for tf=15mn

D: Deposit aspect for tf=20mn

E: Deposit aspect for tf=25mn

F: Deposit aspect for tf=33mn

Fig. 3. Scanning electron micrograph photographs during clogging by soda fluorescein particles.

is higher in the case of a short exposure time. The interesting result means that the filtration process begins with the deposit within the filter bed and comes to an end with the collection on the filter surface. Those conclusions are consistent with the scanning electron micrograph observations.

4.3. *Evolution of filter efficiency during clogging*

The evolution of filter efficiency is shown graphically in Fig. 6. The rise in pressure drop is also plotted in order to link the evolution of both parameters. The effect of particle loading is a great increase of the filter performance which can also be described in two stages. During the first stage corresponding to the small increase of pressure drop, the filter efficiency grows dramatically until the loading point of cake formation is reached, causing the rate of efficiency increase to fall. It turns out to be quite difficult to estimate the following evolution of the efficiency (even for a higher amount of deposited particles) due to a lack of sensibility of the measurement.

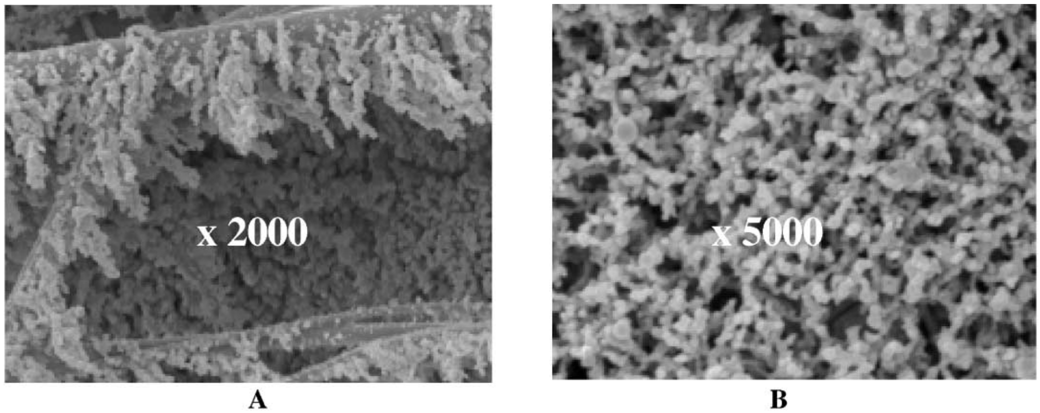

Fig. 4. Dendrites (observation of the filter surface) and particle cake formation (observation of the filter section) (respectively, A and B).

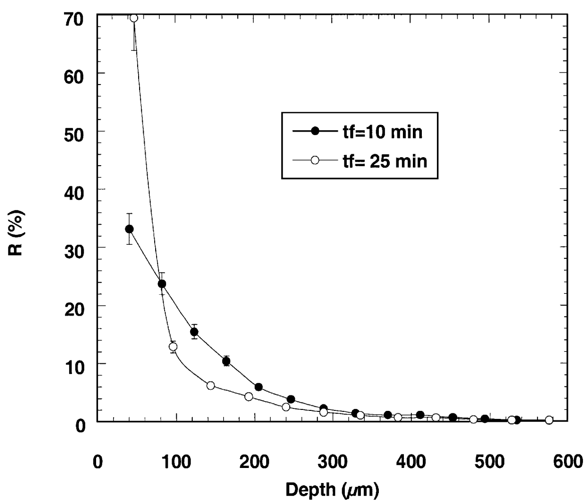

Fig. 5. Penetration profile of soda fluorescein particles inside the filter ($d_p = 0.18$ μm, $C = 3.5$ mg/m^3, $U_0 = 18$ cm/s) for two values of filtration time.

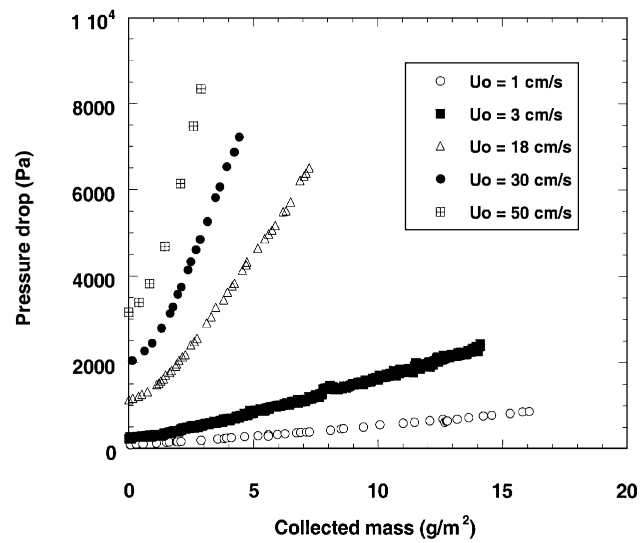

Fig. 7. Evolution of pressure drop for all studied filtration velocities ($d_p = 0.31$ μm).

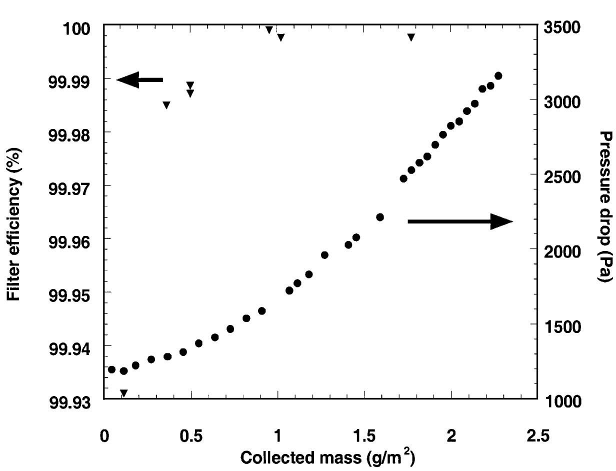

Fig. 6. Evolution of filter efficiency during clogging by soda fluorescein particles ($d_p = 0.18$ μm, $C = 3.5$ mg/m^3, $U_0 = 30$ cm/s).

4.4. Influence of operating conditions

4.4.1. Influence of filtration velocity

Five values of filtration velocity were tested in the range $1 < U_0 < 50$ cm/s corresponding to a laminar flow regime.

The evolution of pressure drop for all studied filtration velocities is plotted in Fig. 7. As can be seen, the slope of the linear part of the curves is greater as the face velocity is high. Nevertheless, in an attempt to test whether this gap between curves was only due to a difference of face velocity or as well to a modification of particle deposition, we plotted the ratio $\Delta P/U_0$ against the deposited mass for all experiments. We can notice that all curves (Fig. 8) are identical. The interesting result means that the way particles settle on the fibres does not depend on filtration velocity (on the range indicated above).

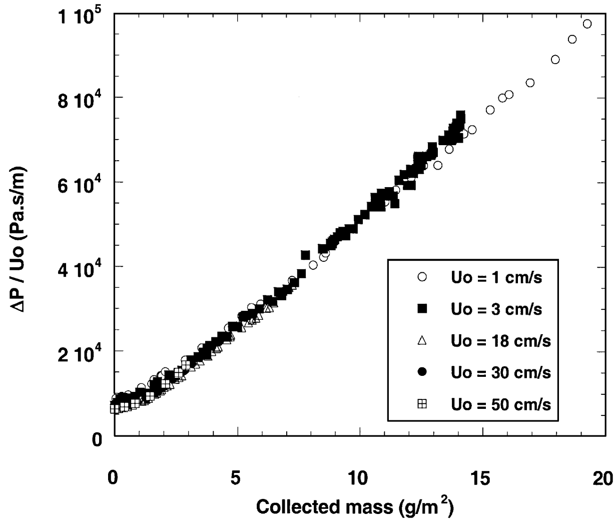

Fig. 8. Evolution of $\Delta P/U_0$ during the clogging by soda fluorescein particles ($d_p = 0.31$ μm).

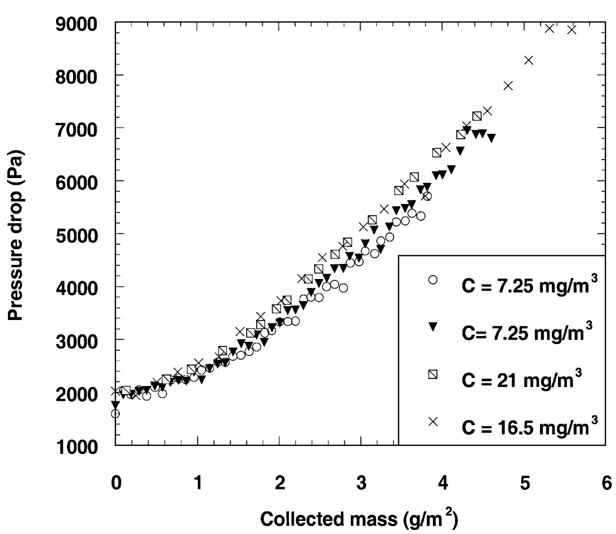

Fig. 9. Influence of upstream aerosol concentration on evolution of pressure drop ($d_p = 0.31$ μm).

4.4.2. *Influence of aerosol concentration*

The aerosol concentration can vary between 5 and 21 mg/m^3 for soda fluorescein particles. The experimental set-up at our disposal does not enable a higher dilution. As illustrated in Fig. 9, on this range of concentrations, no influence was noticed on the evolution of pressure drop.

We also studied the influence of aerosol concentration on the penetration profile. No influence was noticed on the penetration profile either.

That means that the key parameter in filtration process is the mass collected inside the filter whatever be the time needed to achieve it.

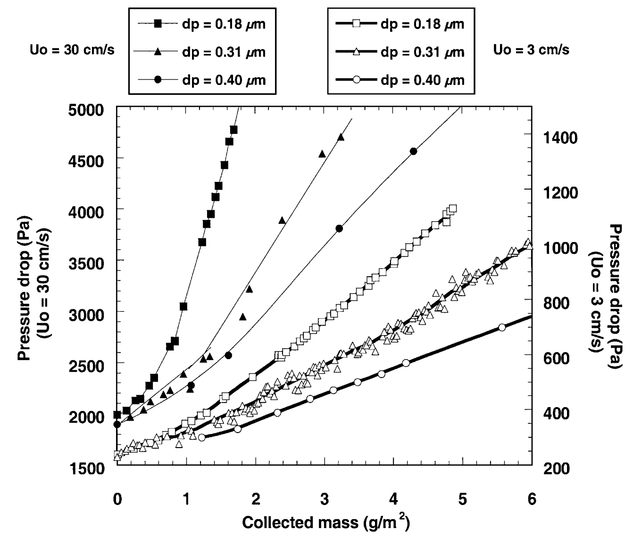

Fig. 10. Influence of particle size on the evolution of pressure drop ($U_0 = 30$ and 3 cm/s).

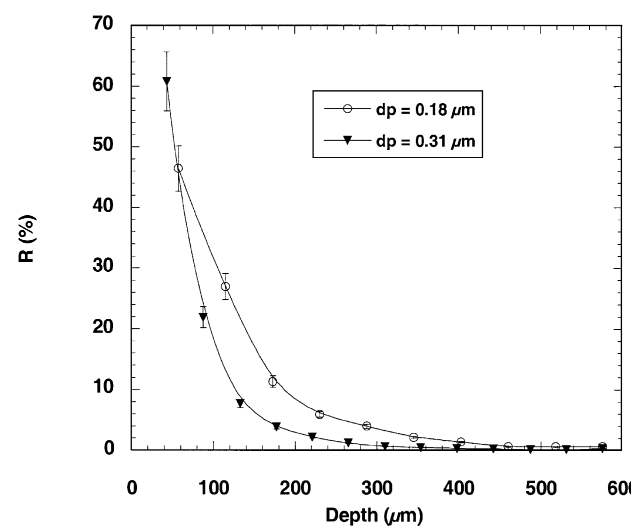

Fig. 11. Influence of particle size on the penetration profile inside the filter ($U_0 = 18$ cm/s, collected mass = 1.5 g/m^2).

4.4.3. *Influence of particle mean size*

Fig. 10 shows the evolution of pressure drop during the filtration of 0.18, 0.31 and 0.4 μm aerosol particles in the case of two face velocities (3 and 30 cm/s). Those curves clearly show that either for a low or high filtration velocity, the pressure drop entailed by aerosol filtration is smaller as particle size is high. This result is linked to the fact that larger particles have a smaller specific area a_g entailing a smaller pressure drop.

In order to examine the influence of particle size on the way that the deposit was built during clogging, we compared the penetration profile of 0.18 and 0.31 μm particles inside the filter for the same operating conditions ($U_0 = 18$ cm/s and collected mass = 1.5 g/m^2). Fig. 11 illustrates graphically this comparison and attests that smaller particles are more penetrating in the depth of the filter.

5. Model

We have developed a new model based on the observation of the clogged filter thanks to scanning electron micrograph. We have already described particle collection as being dendritic deposits (especially in the early stage of filtration). Therefore, we will suppose that all collected particles form dendrites which can be considered as new collecting fibres and contribute to the increase of collection efficiency.

Thus, the filter is divided into various slices in which two kinds of particle collectors coexist: on one hand the fibres of filter, on the other hand deposited particles inside the filter. Slices are characterised by their thickness Z_J. During filtration, each slice J is assumed to be homogeneously loaded by aerosol and packing density of collected particles ($\alpha_{pJ,t}$) depending on the filtration time is calculated as

$$\alpha_{pJ,t} = \frac{\text{Volume of collected particles in slice } J}{\text{Volume of slice } J}. \tag{5}$$

The fractional flow rate crossing the collector made of fibres is assumed to be equal to $1-\alpha_p/(1-\alpha)$ and the one crossing the collector made of dendrites is then $\alpha_p/(1-\alpha)$ (see Fig. 12).

For each time increment and each slice, the particle collection efficiency of fibres and dendrites is calculated according to the already existing models. It consists in the calculation of the individual collection efficiency due to each collecting mechanism (diffusion, interception: η_D, η_R). The individual collection efficiency due to inertia is not here taken into account since this collecting mechanism can be neglected for particle size smaller than 1 μm.

The fibres collection efficiency is then the sum $\eta = \eta_D + \eta_R$. We chose the model developed by Payet (1992)

$$\eta_D = 1,6[(1-\alpha)/Ku]^{1/3} Pe^{-2/3} C_{d_1} C_{d_2}$$

with

$$C_{d_1} = 1 + 0.388\, Kn_f [(1-\alpha)Pe/Ku]^{1/3}, \tag{6}$$

$$C_{d_2} = 1/[1 + 1,6[(1-\alpha)/Ku]^{1/3} Pe^{-2/3} C_{d_1}]$$

and

$$Ku = -0.5 \ln\alpha - 0.75 + \alpha - \alpha^2/4, \tag{7}$$

$$\eta_R = 0.6 \left[\frac{1-\alpha}{Ku} \left(\frac{I^2}{1+I}\right)\right] \left(1 + 1.996\,\frac{Kn_f}{I}\right) \tag{8}$$

with $I = d_p/d_f$.

The filter efficiency is then calculated according to fibres collection efficiency using expression (1).

Then, knowing particle size distribution upstream the filter, it is easy to determine the mass deposited on each slice (collected either on the fibres or on the dendrites), the packing density of collected particles, the diameter of new fibres thanks to the following expressions:

$$m_{fJ,t} = \left(1 - \frac{\alpha_{pJ,t-1}}{1-\alpha}\right) \sum_{i=0}^{n_c} (E_{fJ,i,t} m_{J,t} f_{u_{J,i,t}}) \tag{9}$$

for the mass collected by fibres

$$m_{pJ,t} = \left(\frac{\alpha_{pJ,t-1}}{1-\alpha}\right) \sum_{i=0}^{n_c} (E_{pJ,i,t} m_{J,t} f_{u_{J,i,t}}) \tag{10}$$

for the mass collected by dendrites, where $f_{u_{J,i,t}}$ is the particle fraction upstream layer J, $E_{fJ,i,t}$ and $E_{pJ,i,t}$ are, respectively, the collection efficiency of fibres and particles (dendrites) and are calculated as

$$E_{fJ,i,t} = 1 - \exp\left[\frac{-4\alpha\eta_f Z_J}{\pi(1-\alpha-\alpha_{pJ,t})d_f}\right] \tag{11}$$

and

$$E_{pJ,i,t} = 1 - \exp\left[\frac{-4\alpha_p\eta_p Z_J}{\pi(1-\alpha-\alpha_{pJ,t})d_{PJ,t-1}}\right]. \tag{12}$$

The total efficiency due to both collectors is

$$E_{J,t} = \frac{\sum_{i=0}^{n_c} m_{fJ,i,t} + m_{pJ,i,t}}{m_{J,t}} \tag{13}$$

and the whole mass collected in each layer is $m_{J,t} = (1 - E_{J-1,t})m_{J-1,t}$.

The packing density of collected particles is determined by

$$\alpha_{pJ,t} = \alpha_{pJ,t-1} + \frac{m_{fJ,t} + m_{pJ,t}}{\rho_p Z_J}. \tag{14}$$

The diameter of new fibres is equal to the mean diameter of the collected particles ($\bar{d}_{pJ,t}$) and can be calculated by

$$\bar{d}_{pJ,t} = \frac{\bar{d}_{pJ,t-1}\alpha_{pJ,t-1}\rho_p Z_J + \sum_{i=0}^{n_c}(m_{fJ,i,t} + m_{pJ,i,t})d_{p,i}}{\alpha_{pJ,t-1}\rho_p Z_J + \sum_{i=0}^{n_c}(m_{fJ,i,t} + m_{pJ,i,t})}. \tag{15}$$

The pressure drop across each slice $\Delta P_{J,t}$ is then calculated from modified Bergman's model, the overall pressure drop across the filter is then the sum for all slices.

$$\Delta P_{J,t} = 16\mu U_0 Z_J \left(\frac{4\alpha_{pJ,t}}{\bar{d}^2_{pJ,t}} + \frac{4\alpha}{d_f^2}\right)^{1/2} \left(\frac{2\alpha_{pJ,t}}{\bar{d}_{pJ,t}} + \frac{2\alpha}{d_f}\right) \times (1 + 56(\alpha + \alpha_{pJ,t})^3), \tag{16}$$

$$\Delta P_t = \sum_{J=0}^{n_p} \Delta P_{J,t}. \tag{17}$$

This calculation process is valid for each time increment and enables the prediction of pressure drop during

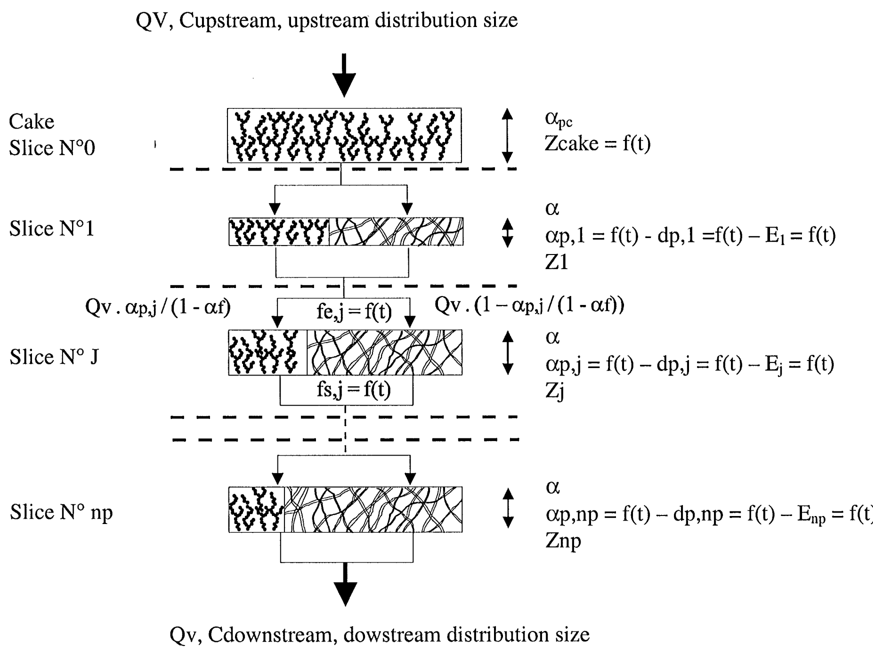

Fig. 12. Schematic diagram of filtration model.

clogging. We had previously examined the validity of this model (only in depth filtration) with several series of experimental data (Thomas et al., 1999).

At each iteration a test is conducted on the packing density of collected particles in the first slice. When α_p reaches limit value $\alpha_{\lim}$ a filter cake begins to grow on the filter surface but depth filtration does continue too. The filter cake is constituted by newly formed dendrites. Their diameter is equal to the dendrite diameter inside the first peeling of the filter (at the beginning of the cake calculation). The pressure drop of the cake is obtained by the application of Novick's law with the packing density of filter cake (α_{pc}) determined by an empirical law as a function of particle diameter. This parameter is assumed to be constant during filtration. The pressure drop is finally summed up to the other elementary pressure drop. Filtration efficiency is calculated in the same way as in depth filtration considering filter cake as a fibrous slice.

5.1. Estimation of filter cake packing density: α_{pc}

The evolution of pressure drop as a function of collected mass shows a linear increasing (during surface filtration). We are able to calculate its slope thanks to different literature experiments.

According to Novick's equation, slope is equal to

$$\text{slope} = \frac{hk\ ag^2 \alpha_{pc}\,\mu}{C_c(1-\alpha_{pc})^3\,\rho_p}\,U_0. \tag{18}$$

Thus, this relation allows us to estimate packing density of filter cake. Fig. 13 shows the evolution of α_{pc} as a function of particle diameter d_p. This evolution can be correlated by

$$\alpha_{pc} = 0.58\left[1-\exp\left(\frac{-d_p}{0.53}\right)\right]. \tag{19}$$

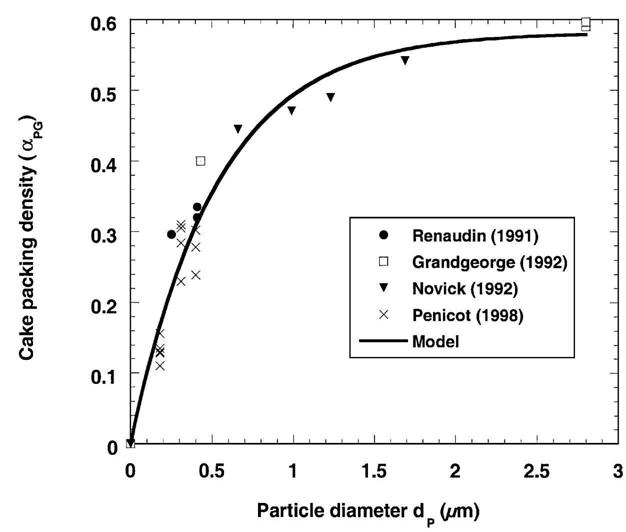

Fig. 13. Evolution of cake packing density as a function of particle diameter.

5.2. Estimation of limit packing density: $\alpha_{\lim}$

During filtration, volume of collected particle V_p in the slice with thickness $\overline{d_p}$ increases. When V_p reaches $V_{p_{\lim}}$

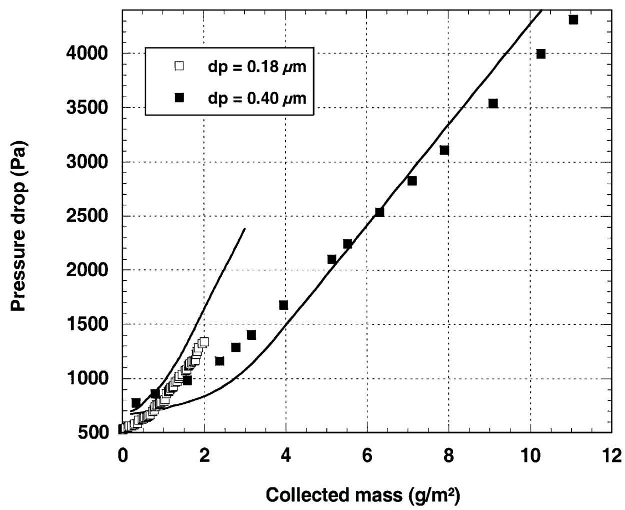

Fig. 14. Comparison of the pressure drop model with experimental results. Filter D309–filtration velocity = 9 cm/s.

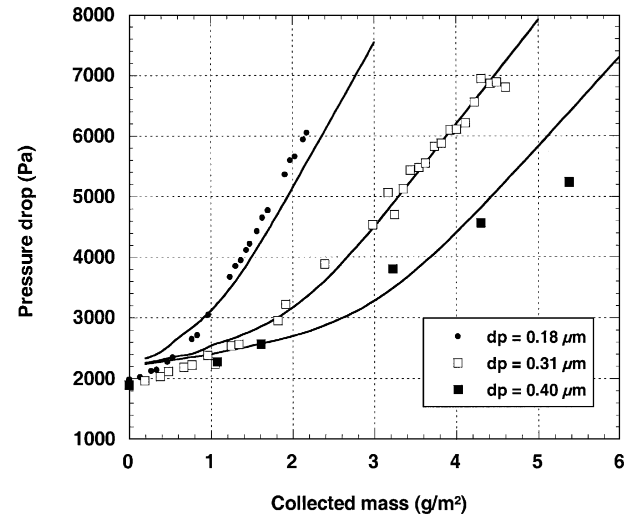

Fig. 16. Comparison of the pressure drop model with experimental results. Filter D309–filtration velocity = 30 cm/s.

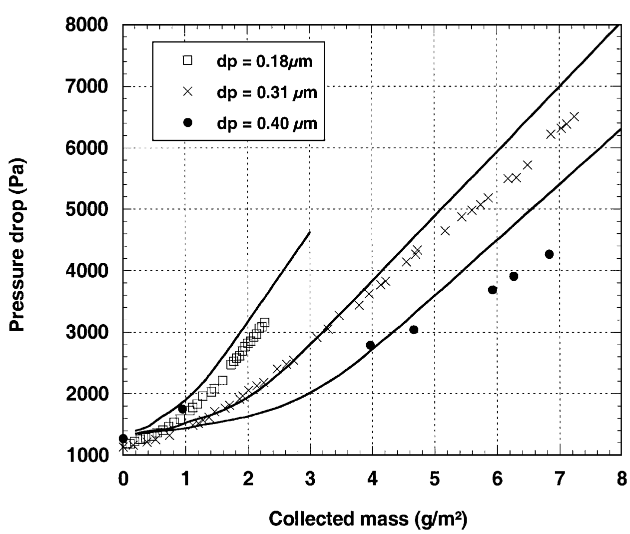

Fig. 15. Comparison of the pressure drop model with experimental results. Filter D309–filtration velocity = 18 cm/s.

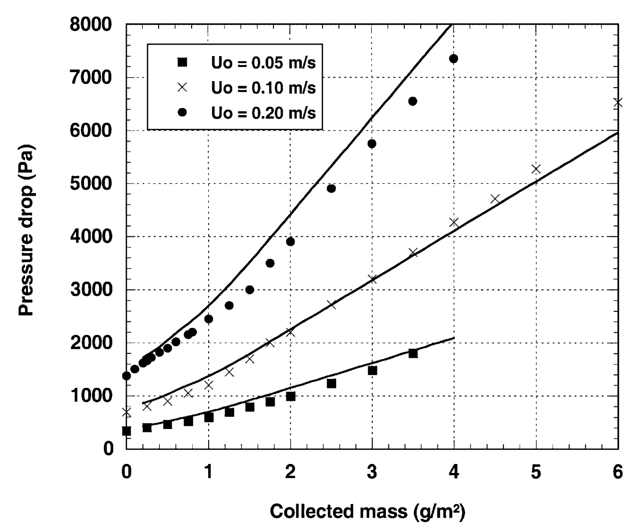

Fig. 17. Comparison of the pressure drop model with experimental results. Filter D306–$d_p = 0.15$ μm.

(Eq. (20)) dendrites start growing out of the filter.

$$V_{p_{\lim}} = \alpha_{pc}(1-\alpha)\Omega_T\overline{d_p} \tag{20}$$

In our model, we define limit packing density $\alpha_{\lim}$ as $V_{p_{\lim}}$ on the volume of first slice.

$$\alpha_{\lim} = \alpha_{pc}\frac{(1-\alpha)}{Z_1}\overline{d_p}. \tag{21}$$

This relation shows that $\alpha_{\lim}$ depends on the particle diameter, cake packing density and filter porosity.

5.3. Comparison with experimental data

Figs. 14–18 show the comparison between model and experimental results. We can notice a good agreement between calculated values and experiments .The optimised parameters of model are: number of slices, $n_p = 10$, number of particle size range, $n_c = 20$ and increment time $= 400$ s.

This model describes very well the transition area between depth filtration and cake filtration. During cake filtration, model and experiment present a stronger difference. This is due to Novick's model. Indeed, this model includes the factor $\alpha_{pc}/(1-\alpha_{pc})^3$ and its numerical value is very sensible to α_{pc}.

Figs. 19 and 20 show, respectively, the influence of particle size and exposure time on the penetration profile for both experiments and models. To begin with, let us note the exponential decrease of the curve obtained with

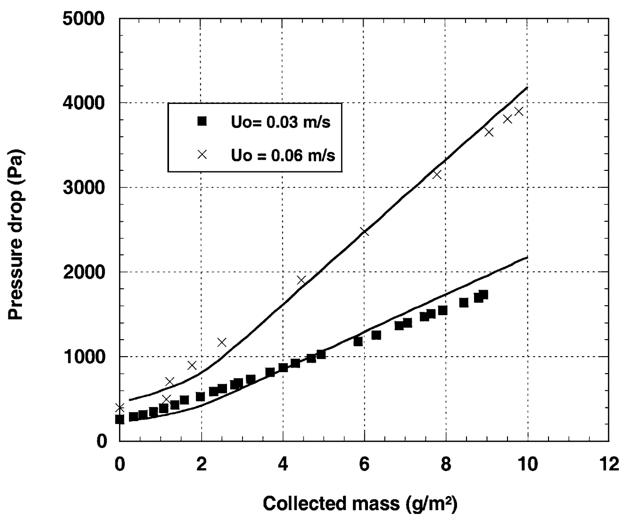

Fig. 18. Comparison of the pressure drop model with experimental results. Filter D306–$d_p = 0.26$ μm.

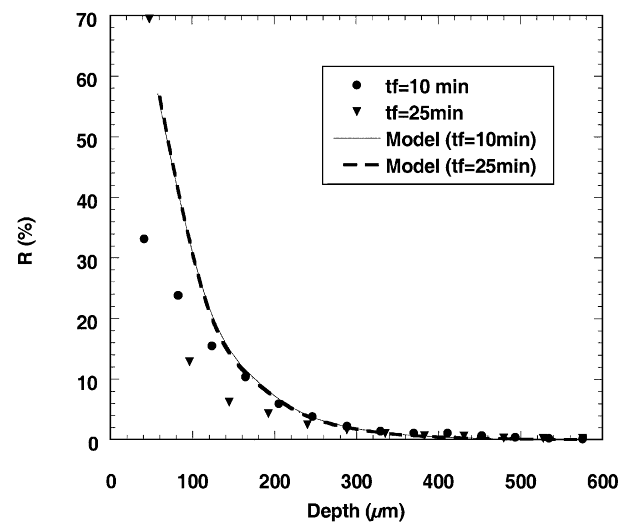

Fig. 20. Comparison between the developed model and penetration profile experimental values: influence of the filtration time ($d_p = 0.18$ μm, $U_0 = 0.18$ m/s).

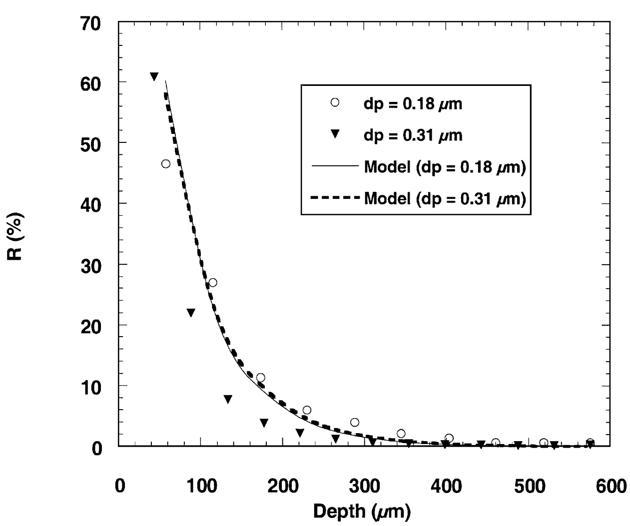

Fig. 19. Comparison between the developed model and penetration profile experimental values: influence of particle size ($U_0 = 0.18$ m/s, collected mass = 1.5 g/m^2).

the model: a result which is consistent with the experimental observations. No influence of either particle size or exposure time is described by the model. It is not a good representation of what really takes place inside the filter.

6. Conclusion

The evolution of pressure drop and filter efficiency of HEPA filters was experimentally described and related to the way that submicronic particles are collected on the fibres for different clogging degrees. The early stage where filtration occurs inside the filter bed is followed by the second step where it mainly occurs on the front edge of the filter. No influence of either the face filtration velocity or the aerosol concentration (on the range studied) on deposit structure was detected. Larger particles were found to entail a smaller pressure drop, which is linked to the specific area.

We can notice a good agreement between model and experiment. Moreover, model very well describes the transition area between the depth filtration and cake filtration. This transition from one type of filtration to another is a continuous process. Model describes also the exponential decrease of penetration profile.

The next work will treat the filter efficiency (comparison between model and experiment) and filtration of micronic particles.

Notation

a_g	particle specific area, 1/m
C	aerosol concentration, mg/m^3 (temperature 0°C and pressure 1.01325×10^5 Pa)
C_c	Cunningham slip correction factor, dimensionless
d_f	mean equivalent fibre diameter, m
d_p	particle diameter, m
$\overline{d_p}$	mean particle diameter, m
E	efficiency, dimensionless
f_u	particle fraction upstream a layer, dimensionless
h_k	Kozeny constant
I	interception parameter, dimensionless
k_2	$=h_k a_g^2 \alpha_{pc} \mu / [C_c(1-\alpha_{pc})^3 \rho_p]$, Pa/m^2/kg

Kn	Knudsen number, dimensionless
Ku	Kuwabara number, dimensionless
m	collected particle mass per filter area unit, g/m^2
n_c	number of particle size range, dimensionless
n_p	number of slices, dimensionless
Pe	Peclet number, dimensionless
U_0	velocity, m/s
Z	total filter thickness, m

Greek letters

α	filter packing density, dimensionless
α_p	packing density of collected particles, dimensionless
α_{pc}	cake packing density, dimensionless
ΔP	filter pressure drop, Pa
ΔP_0	clean filter pressure drop, Pa
η	total single fibre efficiency, dimensionless
η_D	single fibre efficiency for diffusion capture mechanism, dimensionless
η_R	single fibre efficiency for interception capture mechanism, dimensionless
μ	gas dynamic viscosity, Pa s
Ω_T	filtration area, m^2
ρ	density, kg/m^3

Indices

f	relative to fibre
i	index of particle size range
J	slice number
p	relative to particles
t	relative to time

References

Bergman, W., Taylor, R. D., & Miller, H. H. (1978). *15th DOE nuclear air cleaning conference*, *CONF*-780819, Boston.

Billings, C. E. (1966). *Effects of particle accumulation in aerosol filtration*. Ph.D. dissertation, California Institute of Technology, Pasadena, USA.

Brown, R. C. (1993). Theory of airflow through filters modelled as arrays of parallel fibres. *Chemical Engineering Science*, *48*, 3535–3543.

Davies, C. N. (1973). *Air filtration*. London and New York: Academic Press.

Grandgeorges, S. (1992). Etude du colmatage de filtres à fibres par des particules solides. DEA, Institut National Polytechnique de Grenoble, Chambéry, France.

Gougeon, R. (1993). *Filtration des aérosols liquides par des filtres à fibres en régime d'interception et d'inertie.* Ph.D., Université de Paris XII, France.

Happel, J. (1959). Viscous flow in arrays of cylinders. *American International Chemical Engineering Journal*, *5*, 174–177.

Ilias, S., & Douglas, P. L. (1989). Inertial impaction of aerosol particles on cylinders at intermediate and high Reynolds numbers. *Chemical Engineering Science*, *44*, 81–99.

Japuntich, D. A., Stenhouse, J. I. T., & Liu, B. Y. H. (1994). Experimental results of solid monodisperse particle clogging of fibrous filters. *Journal of Aerosol Science*, *25*(2), 385–393.

Juda, J., & Chrosciel, S. (1970). Ein theoretisches Modell der Druckverlusthöhung beim Filtrationsvorgang. *Staub Reinhaltung der Luft*, *5*, 196–198.

Kanaoka, C., & Hiragi, S. (1990). Pressure drop of air filter with dust load. *Journal of Aerosol Science*, *21*, 127–137.

Kirsch, A. A., & Lahtin, U. B. (1975). Gas flow in high porous layers of high dispersed particles. *Journal of Colloid and Interface Science*, *52*, 270–276.

Kirsch, A. A., & Stechkina, I. B. (1977). Inertial deposition of aerosol particles in model filters at low Reynolds numbers. *Journal of Aerosol Science*, *8*, 301–307.

Kuwabara, S. (1959). The forces experienced by randomly distributed parallel circular cylinders or spheres in viscous flow at small Reynolds numbers. *Journal of the Physical Society of Japan*, *14*, 527–532.

Lajos, T. (1985). The effect of inhomogenity on flow in fibrous filters. *Staub Reinhaltung der Luft*, *45*, 19–22.

Letourneau, P., Mulcey, Ph., & Vendel, J. (1990). Aerosol penetration inside HEPA filtration media. *21st DOE/NRC nuclear air cleaning conference, CONF*-900813, San Diego.

Lee, K. W., & Liu, B. Y. (1982). Theoretical study of filtration by fibrous filters. *Aerosol Science and Technology*, *1*, 147–161.

Liu, B. Y., & Rubow, K. L. (1990). Efficiency, pressure drop and figure of merit of high efficiency fibrous and membrane filter media. *Proceedings of the fifth world filtration congress*, Nice, Vol. 3 (pp. 112–119).

Nagel, F., & Buggish, H. (1996). Low Reynolds number flow fields in imperfect fibre arrangements. *Powder Technology*, *86*, 7–20.

Natanson, G. L. (1987). *Filtration, principles and practices*. New York: Marcel Dekker.

Novick, V. J., Higgins, P. J., Dierkschiede, B., Abrahamson, C., Richardson, W. B., Monson, P. R., & Ellison, P. G. (1990). Efficiency and mass loading characteristics of a typical HEPA filter media material. *Proceedings of the 21st DOE/NRC nuclear air cleaning conference*, San Diego (pp. 782–798).

Payatakes, A. C., & Gradon, L. (1980). Dendritic deposition of aerosols by convective brownian diffusion for small, intermediate and high particle Knudsen numbers. *American International Chemical Engineering Journal*, *26*, 443–454.

Payatakes, A. C., & Okuyama, K. (1982). Effects of aerosol particle deposition on the dynamic behavior of uniform or multilayer fibrous filter. *Journal of Colloid and Interface Science*, *88*(1), 55–78.

Payet, S., Boulaud, D., Madelaine, G., & Renoux, A. (1992). Penetration and pressure drop of a HEPA filter during loading with submicron liquid particles. *Journal of Aerosol Science*, *7*, 723–735.

Penicot, P. (1998). *Etude de la performance de filtres à fibres lors de la filtration d'aérosols liquides ou solides submicroniques*. Ph.D., Institut National Polytechnique de Lorraine, Nancy. France.

Ramarao, B. V., Tien, C., & Mohan, S. (1994). Calculation of single fiber efficiency for interception and impaction with superposed brownian motion. *Journal of Aerosol Science*, *25*, 295–313.

Renaudin, V. (1991). Modélisation du colmatage de filtres à fibres. DEA, Institut National Polytechnique de Grenobles, Chambéry, France.

Schmidt, E., & Löffler, F. (1990). The analysis of dust cake structures. *Particle and Particle System Characterization*, *8*, 105–109.

Spielman, L., & Goren, S. L. (1968). Model for predicting pressure drop and filtration efficiency in fibrous media. *Environmental Science and Technology*, *2*, 279–287.

Stechkina, I. B., Kirsch, A. A., & Fuchs, N. A. (1969). Investigations of fibrous filters for aerosols calculation of aerosol deposition in model filters in the region of maximum particle breakthrough. *Colloid Journal of the USSR*, *31*, 97–101.

Suneja, S. K., & Lee, C. H. (1974). Aerosol filtration by fibrous filters at intermediate Reynolds numbers (<100). *Atmospheric Environment*, *8*, 1081–1084.

Thomas, D., Contal, P., Renaudin, V., Penicot, P., Leclerc, D., & Vendel, J. (1999). Modelling pressure drop in HEPA filters during dynamic filtration. *Journal of Aerosol Science*, *30*(2), 235–246.

Vendel, J., Letourneau, P., & Renaudin, V. (1992). Effects of the particle penetration inside the filter medium on the HEPA filter pressure drop. *Proceedings of the 22nd DOE/NRC nuclear air cleaning conference*, *CONF*-920823, Denvers.

Witten, T., & Sander, L. (1983). Diffusion-limited aggregation. *Physical Review*, *27*, 5686.